

Figure S1 Selection of imaging (A,B) and clinical features (C,D) using the LASSO logistic regression algorithm for prediction of LNM. The penalization coefficient λ in the LASSO model was tuned using 10-fold cross-validation and minimum criterion for presence of LNM. The lower X-axis shows $\log(\lambda)$, while the top X-axis indicates the number of predictors for the given $\log(\lambda)$. The Y-axis indicates binomial deviance. Red dots represent average misclassification errors for every model with given λ , and the vertical bars indicate the upper and lower values of the misclassification errors. The vertical black lines define the optimal λ , which provides its best fit to the data. As a result, an optimal λ of 0.017, with $\log(\lambda) = -4.085$, was selected for LNM prediction using clinical features, and an optimal λ of 0.025, with $\log(\lambda) = -3.674$, was selected for LNM prediction using imaging features. LASSO, least absolute shrinkage, and selection operator; LNM, lymph node metastasis.

Table S1 Formulas for imaging scores and clinical scores in the LASSO models for MVI, satellite nodules and LNM status

Group	Formula
Imaging scores for MVI status	$-0.25394 \times \text{shape: globular} + 0.59647 \times \text{targocid restriction: absent} - 0.069 \times \text{arterial enhancement pattern: global} - 0.76723 \times \text{peritumoral enhancement pattern: none} + 0.10008 \times \text{peritumoral enhancement pattern: wedge} - 0.68747 \times \text{washout: absent} - 0.36876 \times \text{false capsule: none} + 0.05932 \times \text{false capsule: incomplete} - 0.06953 \times \text{bile duct dilation: absent} - 0.09913 \times \text{surface retraction: absent} + 0.1107 \times \text{nodule in nodule architecture: absent} - 0.43829 \times \text{LR-RADS categorization: LR-3} + 0.88054 \times \text{LR-RADS categorization: LR-TIV} - 0.036$
Imaging scores for satellite nodules status	$-0.50598 \times \text{shape: globular} - 0.18084 \times \text{hemorrhage: absent} + 0.46096 \times \text{targetoid restriction: absent} - 0.6319 \times \text{peritumoral enhancement pattern: none} + 0.11745 \times \text{peritumoral enhancement pattern: wedge} - 1.36412 \times \text{false capsule: none} + 0.18161 \times \text{false capsule: incomplete} - 0.22098 \times \text{bile duct dilation: absent} - 0.75007 \times \text{surface retraction: absent} - 0.61861 \times \text{mosaic architecture: absent} - 0.350$
Imaging scores for LNM status	$1.42052 \times \text{shape: irregular} - 0.82546 \times \text{arterial enhancement pattern: global} + 0.46018 \times \text{peritumoral enhancement pattern: irregular} + 0.61432 \times \text{washout: absent} + 0.15252 \times \text{corona enhancement: absent} - 3.167$
Clinical scores for LNM status	$0.52543 \times \text{tumor number: solitary} + 0.34521 \times \text{hepatitis B virus: negative} - 0.30251 \times \text{PLR: PLR} < 76.74 + 0.70132 \times \text{AAPR: AAPR} < 0.53 + 0.12387 \times \text{total bilirubin: total bilirubin} < 17.1 - 0.14724 \times \text{AST: AST} < 45 - 0.35364 \times \text{CA19-9: CA19-9} < 37 - 2.98345$

LASSO, least absolute shrinkage, and selection operator; MVI, microvascular invasion; LNM, lymph node metastasis; LI-RADS, Liver Imaging Reporting and Data System; PLR, platelet to lymphocyte ratio; AAPR, albumin-to-alkaline phosphatase ratio; AST, aspartate aminotransferase; CA 19-9, carbohydrate antigen 19-9.

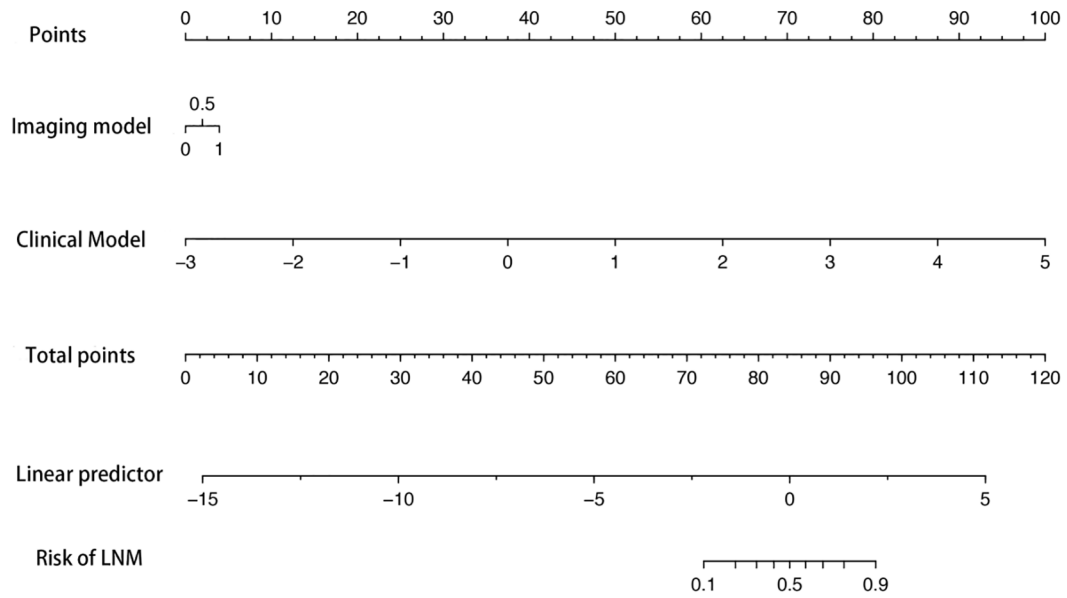


Figure S2 Nomogram for predicting the presence of LNM. Points are assigned for clinical model and imaging model for predicting the presence of LNM. LNM, lymph node metastasis.

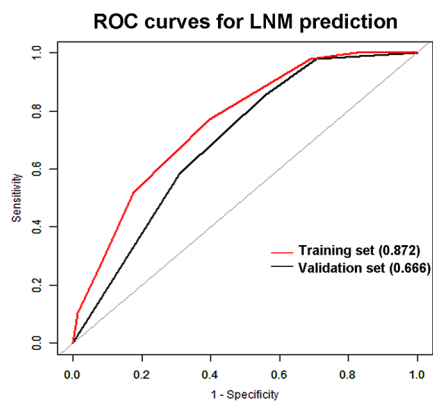


Figure S3 Receiver operating curve for predicting the LNM in the training set (A) and validation set (B) set using the combination nomogram. ROC, receiver operating characteristic; LNM, lymph node metastasis.

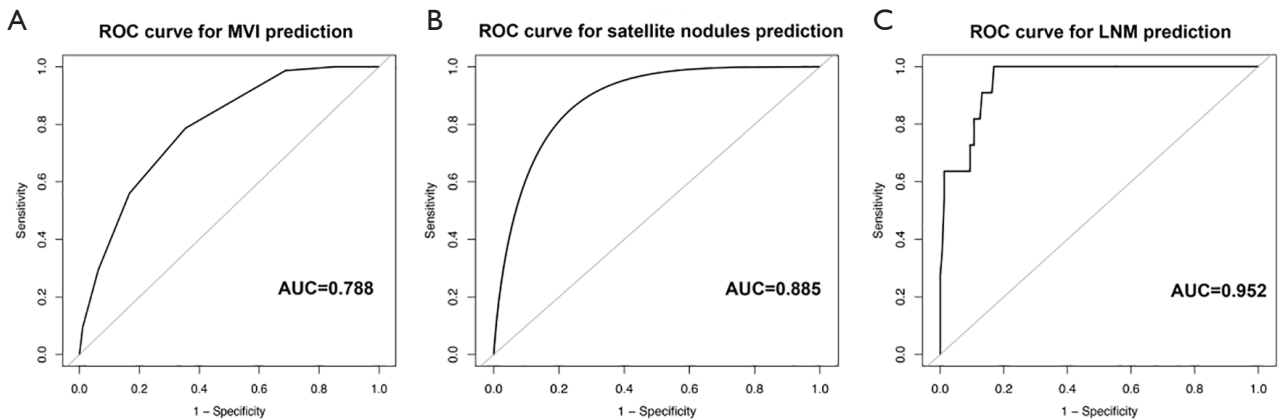


Figure S4 Receiver operating curve for predicting the MVI (A), the presence of satellite nodules (B) and LNM (C) in the CHCC-CCA subtype. ROC, receiver operating characteristic; MVI, microvascular invasion, LNM, lymph node metastasis; CHCC-CCA, combined hepatocellular cholangiocarcinoma.

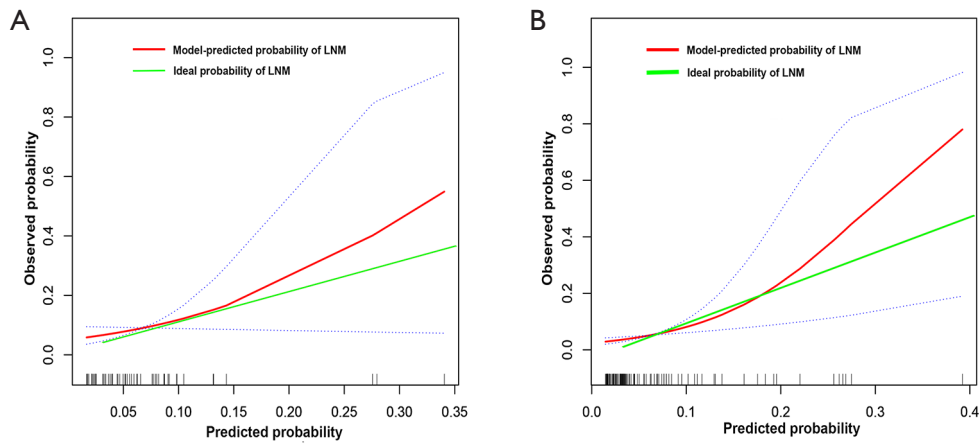


Figure S5 The calibration curves of the combination nomogram for prediction of LNM in the training set (A) and validation set (B). LNM, lymph node metastasis.

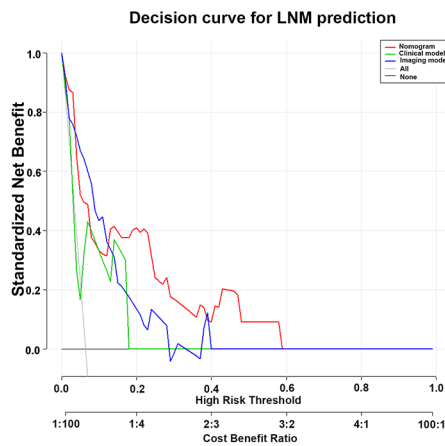


Figure S6 The decision curves of the combination nomogram, clinical model, and imaging model for prediction of LNM in overall patients. Vertical axis: the net benefit; horizontal axis: the threshold probability at a range of 0.0 to 1.0. The gray line represents the decision curve of the assumption that all patients suffer from LNM; the black line represents the decision curve of the assumption that no patients suffer from LNM. ROC, receiver operating characteristic; MVI, microvascular invasion; LNM, lymph node metastasis.